University of Baghdad
College of Engineering
JOURNAL OF ENGINEERING

Journal of Engineering
journal homepage: www.joe.uobaghdad.edu.iq
Number 5 Volume 26 May 2020

Chemical, Petroleum and Environmental Engineering

Building 1D Mechanical Earth Model for Zubair Oilfield in Iraq

Aows Khalid Mohammed *
University of Baghdad
Baghdad, Iraq
Aows.khalid@coeng.uobaghdad.edu.iq

Nada Sabah Selman
University of Baghdad
Baghdad, Iraq
nadaszubaidi@yahoo.com

ABSTRACT

Many problems were encountered during the drilling operations in Zubair oilfield. Stuckpipe, wellbore instability, breakouts and washouts, which increased the critical limits problems, were observed in many wells in this field, therefore an extra non-productive time added to the total drilling time, which will lead to an extra cost spent. A 1D Mechanical Earth Model (1D MEM) was built to suggest many solutions to such types of problems. An overpressured zone is noticed and an alternative mud weigh window is predicted depending on the results of the 1D MEM. Results of this study are diagnosed and wellbore instability problems are predicted in an efficient way using the 1D MEM. Suitable alternative solutions are presented ahead to the drilling process commences in the future operations.

Keywords: Oilfield, Mechanical Earth Model, Wellbore Instability, NonProductive Time Reduction, Pore Pressure Prediction.

بناء نموذج جيوميكانيكي ارضي احادي البعد لحقل الزبير النفطي في العراق

ندى صباح سلمان
جامعة بغداد

اوس خالد محمد
جامعة بغداد

الخلاصة

العديد من المشاكل واجهتها عمليات حفر الابار في حقل الزبير النفطي. استعصاء الانابيب, عدم ثبوتية جدران الابار, توسع و اجتراف في جدران تجاويف الابار هي احدى ابرز هذه المشاكل. ساهمت هذه المشاكل بزيادة الوقت الغير منتج وبالتالي صرف و خسارة مبالغ اضافية. تم بناء نموذج ارضي جيوميكانيكي احادي البعد لتشخيص المشاكل و اقتراح حلول ملائمة لهذا النوع من المشاكل. بناءا على نتائج النموذج, تم تشخيص منطقة ذات ضغط مسامي عالي و بالتالي تم بناء برنامج سائل حفر بديل عن المستخدم الحالي لتفادي المشاكل الممكنة في هذه المنطقة. نتائج هذه الدراسه شخصت و توقعت حدوث المشاكل في الابار المدروسة بطريقة كفوءة و تم مطابقتها مع نتائج مقاسة. بأستخدام نتائج هذا النموذج, تم ايجاد و اقتراح حلول ملائمة و مناسبة لتفادي هكذا نوع من المشاكل اثناء عمليات تطوير الحقول و حفر ابار مستقبلية.

الكلمات الرئيسية: حقل الزبير النفطي, نموذج ارضي جيوميكانيكي, عدم ثبوتية الابار, تقليل الوقت الغير منتج, توقع الضغط المسامي.

*Corresponding author
Peer review under the responsibility of University of Baghdad.
https://doi.org/10.31026/j.eng.2020.05.04

Article received: 14/4/2019
Article accepted:13/7/2019
Article published:1/5/2020

1. INTRODUCTION

Zubair Oilfield is located in the southern part of Iraq as shown in **Fig. 1** and discovered in 1947. It is one of the most prolific oilfields in Iraq. The geologic column for Zubair oilfield is viewed in **Fig.2.** Non-productive time (NPT) is observed almost in most of the wells in Zubair oilfield, especially in the selected wells which is shown in **Fig. 3** and almost 80% of the total NPT was due to the wellbore instability problems.

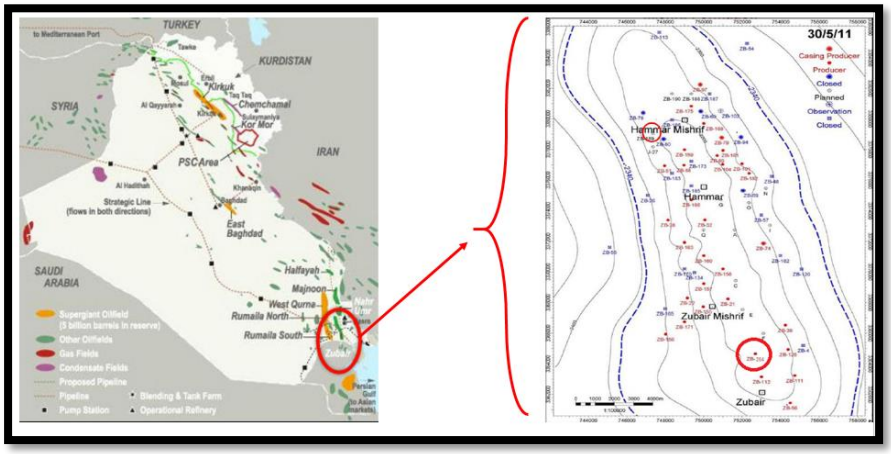

Figure 1. Location Map of Zubair Oilfield and the two selected wells.

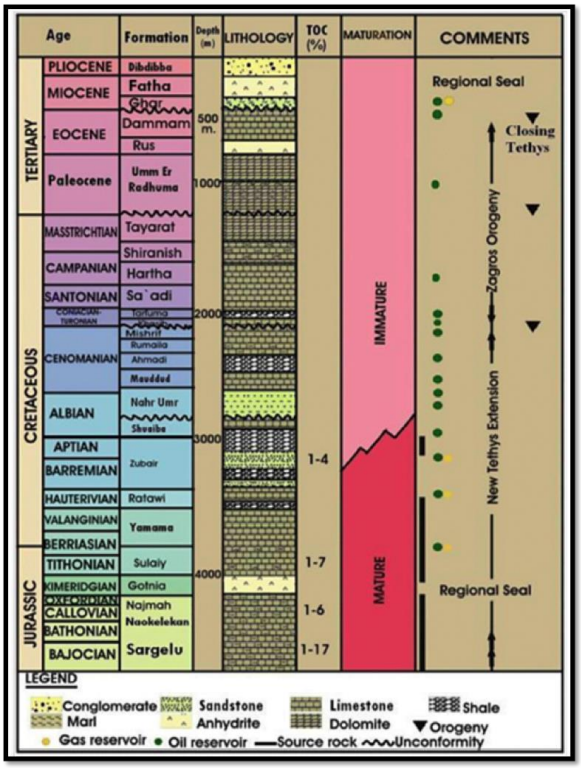

Figure 2. Geologic column of Zubair oilfield, **(AlKhafaji, 2003)**.

The mechanical earth modeling process is presenting the numerical values of the mechanical rock properties and the stress state for a certain geologic or stratigraphic column in a certain field.

(Fischer, 2013) studied and evaluated the potential and importance of building a MEM on predicting the in situ stresses in reservoir scale.

Utilizing the managed pressure drilling (MPD) in narrow mud window and abnormal pore pressure situations is the best candidate. A study by **(Alkamil and Abbood, 2018)** on utilizing the MPD in nearby Iraqi oilfield gave good results. Lack of data is always an issue in the process of mechanical earth modeling if not compensated by a robust tool; the process will be a waste of time. **(Sirat, et al., 2015)** investigated the lack of calibration data on the MEM construction process. They highlighted the importance of the availability of the complete sets to construct a reliable MEM. **(Goodman and Connolly, 2007)** also studied the importance and the value of the data and calibration values in the process of constructing a MEM.

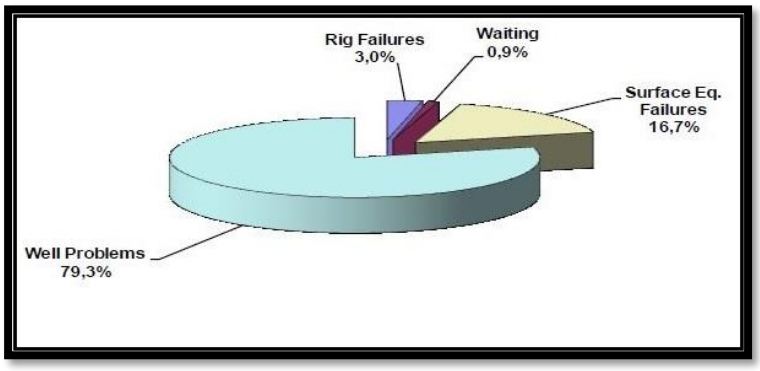

Figure 3. Total NPT breakdown, Zubair oilfield drilling reports.

A mechanical earth model (MEM) was built from an offset wells to determine the safe mud window in the predrill phase, **(Plumb, et al., 2000)**. A comprehensive study was carried out by building a 1D MEM in vertical well in the Persian Gulf, which showed an interference between the modeled profiles of the stresses and the breakouts and their effects on wellbore instability, **(Kidambi and Kumar, 2016)**.

(Amani, et al., 2010) utilized different logging data to construct a 1D MEM to a mature oil field. They used the constructed MEM to predict the safe mud weight window and possible problems and suggested an alternative drilling program.

(Gholami, et al., 2014) studied the mud window determination. They came to a conclusion that picking the pore pressure as the lower limit and the fracture gradient as the upper limit, gave good results in vertical wells. **(Fattahpour, et al., 2012)** constructed a 1D MEM for one well in southwest Iran and applied the model to design the best mud weight program strategy. **(Moazzeni, et al., 2010)** made the best utilization of log and drilling data to construct a MEM and their results showed a significant decrease in the NPT.

Ahead of the drilling process started, mechanical earth modeling should be made since it is one of the essential elements in reducing the non-productive time because it assesses and evaluates all the necessary problems and parameters that occurred in nearby wells therefore, it enables us to utilize those solutions to drill new wells safely.

Non-productive time related to the drilling problems in Zubair Oilfield is estimated to be 79.3%. This percentage considered high. Therefore, it is necessary to reduce this value by assessing the root problems that causes time to increase.

2. PRINCIPLE STRESSES:

The state of stress can be evaluated by determining at least four parameters: overburden stress, Sv; the maximum horizontal stress (SHmax); minimum horizontal stress (Shmin) and orientation of one of the stresses such as azimuth of the maximum horizontal stress.

2.1 Overburden Stress:

The overburden stress (Sv) generated by the weight of the overlying layers. Bulk density log is the source for calculating the overburden stress using Eq. (1). However, in most cases, the upper interval is not logged, therefore; linear extrapolation is used for calculating the overburden stress in the upper unlogged interval.

$$\sigma v = \int_0^Z \rho(z) * g * dz \quad (1)$$

where,

σv is the overburden stress, (Pa), $\rho(z)$ is the bulk density log at depth z, (kg/m^3), g, is the constant of gravitational acceleration = 9.81 (m/s^2), z is the depth at the depth of interest, (m).

2.2 Pore Pressure Prediction:

Analysis of pore pressure workflow performed by utilizing well logging data (Resistivity and Acoustic logs) and calibrated with measured values obtained by reservoir characterization tool (RCT). A reasonable match is obtained from modeled profile with the measured values for both wells.

Due to the successive bedding of sandstone and shale in addition to carbonates in both wells, Eaton sonic model is used to model the pore pressure profile, Eq. (2). An increase in the profiles noticed in one of the wells at Tanuma formation, which gave a narrow mud window and difficult drilling scenario.

$$Pp = S - \left[(S - P_{NCT}) \left(\frac{X_{NCT}}{X_{obs}} \right)^3 \right] \quad (2)$$

where,

Pp is the pore pressure, psi.

S is the overburden stress, psi.

P_{NCT} is the hydrostatic pressure value, psi

X_{NCT}, Xobs are the sonic log reading on the normal compaction trend line and on the log curve respectively, sec/ft.

2.3 Horizontal Stresses:

2.3.1 Magnitude of Minimum Horizontal Stress, Shmin:

Several methods are available to determine the magnitude of the minimum horizontal stress. Leak-off test and extended leak-off test are the most reliable methods if available. An alternative to these methods is to model the minimum horizontal stress using well logs by using stress contrast method which also known as Eaton equation, Eq. (3)

$$Shmin = \left(\frac{\vartheta}{1-\vartheta} \right) (Sv - Pp) + Pp \quad (3)$$

where,

ϑ is the Poisson ratio.

Sv is the overburden stress, psi, Pp is the pore pressure, psi.

2.3.2 Orientation of the Minimum Horizontal Stress:

Direction of the minimum horizontal stress can be specified from the available XRMI image logs. In vertical wells, breakouts occur in the same direction or parallel to the minimum horizontal stress where the maximum compressive shear stress localize.

2.3.3 Maximum Horizontal Stress, (SHmax)
2.3.3.1 Magnitude of Maximum Horizontal Stress:

Three methods are used to estimate the magnitude of the maximum horizontal stress, the effective stress method, the stress contrast method and the equilibrium ratio method.

The effective stress ratio method requires calibration points, which were taken from a study on a near field. It calculates the ratio at the depth of calibration points and then interpolates the maximum horizontal stress profile for the rest of the interval using Eq. (4).

$$ESRmax = \left(\frac{\text{Shmax}-\text{Pp}}{Sv-Pp}\right) \quad (4)$$

The stress contrast method calculates the maximum horizontal stress from well logs using Eq. (5) providing that the tectonic strain is in the maximum horizontal stress direction.

$$SHmax = \left(\frac{\vartheta}{1-\vartheta}\right)(Sv - Pp) + Pp + \left(\frac{1+\vartheta}{1-\vartheta^2}\right)E\varepsilon \quad (5)$$

where, $\varepsilon = 5\times10^{-5}$

The equilibrium ratio method calculates the maximum horizontal stress magnitude based on the three stress states. According to the geological reports, stress state is in normal faulting mode, (Sv > SHmax > Shmin) and choosing the default ratio of 0.5 and using Eq. (6) and rearranging to solve for SHmax.

$$\left(\frac{\text{SHmax}-\text{Shmin}}{Sv-Shmin}\right) = 0.5 \quad (6)$$

2.4 Rock Mechanical Properties:

Understanding of the mechanical properties of the rocks is of an extreme importance in drilling and stability issues. Two types of rock mechanical properties, which are; the static and dynamic, are available. The static properties usually measured in the laboratory tests and they used to compare their values with the log-derived dynamic properties.

Due to the absence of any laboratory tests, static rock mechanical properties, estimated from correlations that relates dynamic properties.

Rock mechanical properties include rock strength properties (unconfined compressive strength, UCS), coefficient of internal friction, and elastic properties (young modulus and Poisson ratio).

2.4.1 Dynamic Properties:
2.4.1.1 Poisson ratio:

Dynamic Poisson ratio is estimated using Eq. (7).

$$\vartheta_{dyn} = \frac{Vp^2 - 2Vs^2}{2(Vp^2 - Vs^2)} \quad (7)$$

where,

ϑ is Poisson ratio.

V_p is the compressional wave velocity, km/s.

V_s is the shear wave velocity, km/s

2.4.1.2 Young Modulus (E_{dyn}):

Young modulus is estimated using Eq. (8).

$$E_{dyn} = \rho\, V_s^2 \frac{3Vp^2 - 4Vs^2}{(Vp^2 - Vs^2)} \quad (8)$$

where,

E_{dyn} is the dynamic Young modulus, MPsi.

ρ is bulk density log reading, gm/cm^3.

2.4.2 Static Properties:

2.4.2.1 Poisson ratio:

A correlation is made on a nearby field between lab test and the log-derived (dynamic) Poisson ratio to model the static Poisson ratio using Eq. (9).

$$\vartheta_{static} = 0.8834 * \vartheta_{dyn} \quad (9)$$

2.4.2.2 Young Modulus:

The generalized Lacy correlation 1997, Eq. (10) is used to convert from the dynamic to the static Young modulus.

$$E_{static} = 0.018E_{dyn}^2 + 0.422E_{dyn} \quad (10)$$

2.5 Strength Rock Properties:

2.5.1 Unconfined Compressive strength (UCS):

Due to the different lithology types in each well, UCS estimated from four correlations according to each lithology as listed in **Table 1**.

Table 1. UCS correlations for different lithology

Lithology	**UCS Correlation, MPa**	
Sandstone	$UCS = 185165\, e^{-0.037*\Delta T}$	McNally, 1987
Limestone	$UCS = 23018 * e^{-4.79*NPHI}$	Qatif-Nphi, 1992
Dolomite	$UCS = 64 * E^{0.34}$	Jizba, 1991
Shale	$UCS = 2.12 * e^{9} * \Delta T^{-2.93}$	Horsrud, 2007

where,

ΔT is the compressional slowness log in μs/ft.

NPHI is the neutron porosity log, fraction.

E is the static Young modulus, MPsi.

2.5.2 Internal Friction coefficient (μ):

The generalized Lal-Vp correlation used to calculate the internal friction coefficient in four types of lithology is given by Eq. (11).

$$\mu = \tan\left(\arcsin\left(\frac{V_p - 1}{v_p + 1}\right)\right) \quad (11)$$

3. The Results

3.1 Rock Mechanical Properties:

Dynamic mechanical properties are calculated using the correlations listed above. Due to the absence of any rock lab experiments, the dynamic properties converted to the static properties using the available studies on the nearby field's correlations **(Fig. 4a and 4b)**.

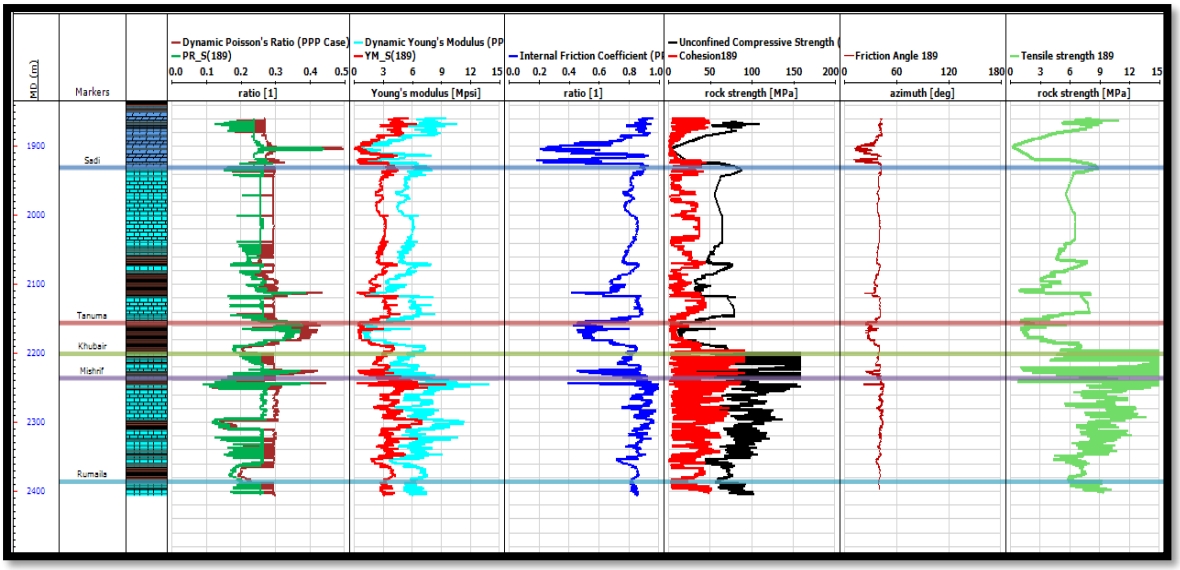

Figure 4a. Rock Mechanical Properties in well ZB 189.

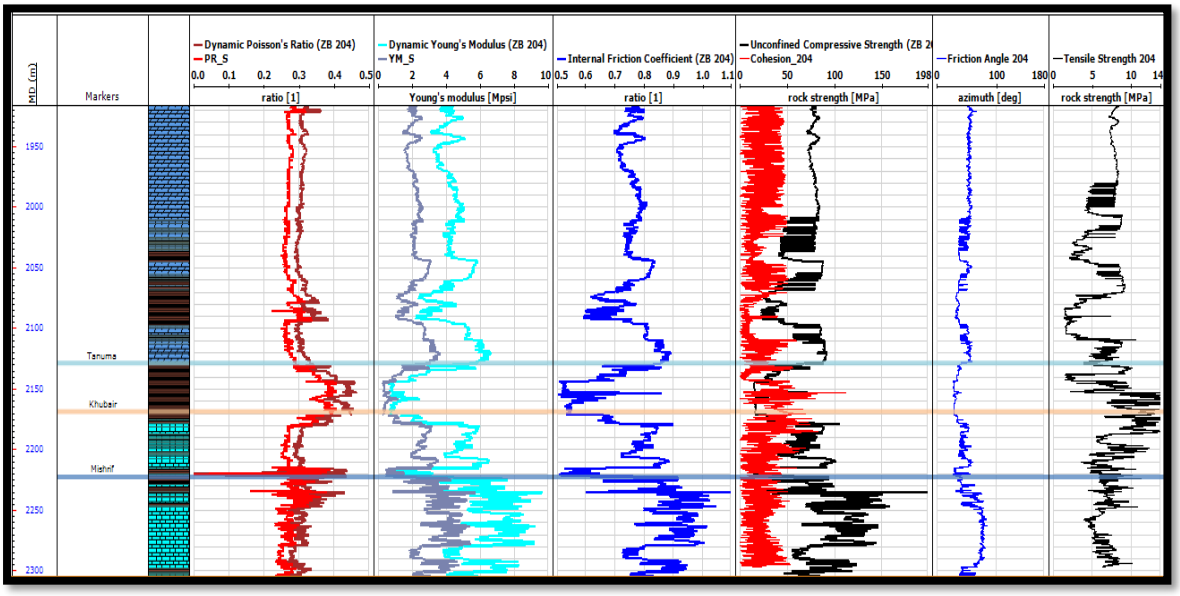

Figure 4b. Rock Mechanical Properties in well ZB 204.

3.2 In-Situ Stresses Magnitudes:

3.2.1 Overburden stress:

Density log is available (from 1850.38 to 2440.21 m) in ZB 189 and (from 1882.38 to 2442.21 m) in ZB 204 therefor, linear extrapolation was needed to accommodate for the missing density curve in the upper interval part of the well. Then, the overburden stress calculated using Eq. (1) and given in **(Fig. 5a and 5b)**.

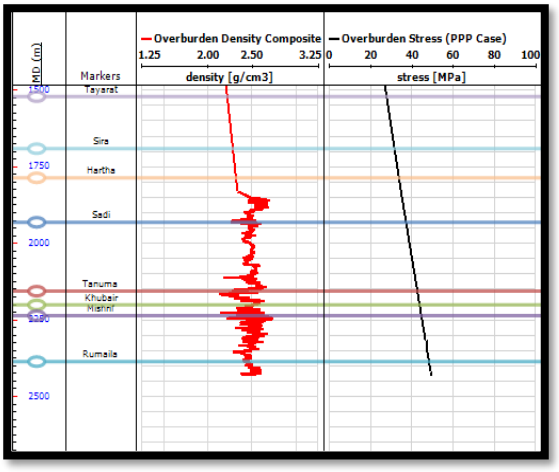

Figure 5a: Density log and overburden stress in well ZB 189**.**

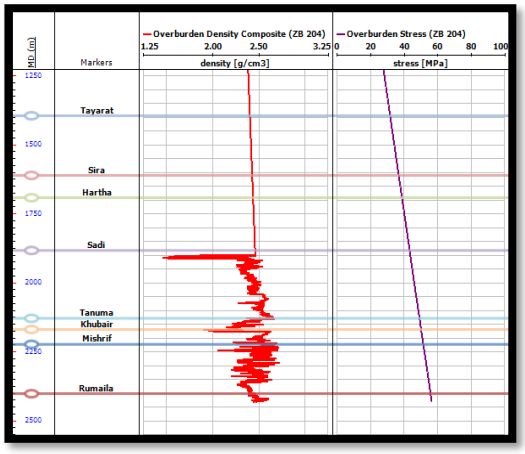

Figure 5b: Density log and overburden stress in well ZB 204.

3.2.2 Pore Pressure:

Pore pressure in both wells **(Fig. 6a and 6b)** predicted from both acoustic and resistivity log sets, and a very good match in well ZB 204 is obtained from acoustic log with the measured pore pressure

(red points in both plots) and a good match in ZB 189 from Weatherboards' RCT (Reservoir Characterization tool).
Due to the undesired results from the resistivity logs, pore pressure prediction from resistivity log is ignored, and a reliable pressure profile from sonic log adopted in the consequent calculations.
Due to the limited data of the pressure measurements in ZB 204, the measured pressure points are used as a calibration points in ZB 189 as well since both wells are in the same geological settings and completed at the same time.

3.2.3 Horizontal Stresses Magnitude:

Horizontal stress profiles **(Fig. 7a and 7b)** in both wells modeled using two different methods, the effective stress method and the stress contract method.
In the effective stress method, calibration points are taken from a previous study (Abbood, 2016) on a nearby field because no leak-off tests available. This method calculates the effective stress ratio (ESR) using Eq. (12a) and Eq. (12b)

$$\text{ESRmin} = \frac{S_{hmin-P_p}}{S_{V-P_p}} \quad (12a)$$

$$\text{ESRmax} = \frac{S_{Hmax-P_p}}{S_{V-P_p}} \quad (12b)$$

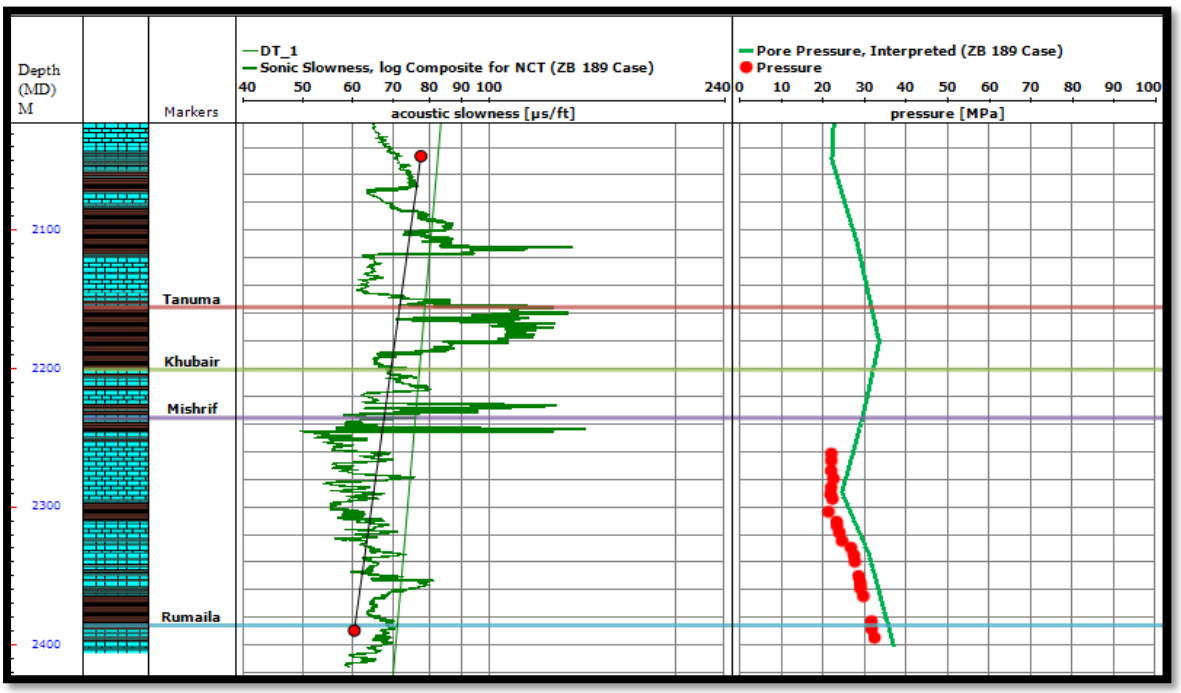

Figure 6a. Pore pressure profile in well ZB 189.

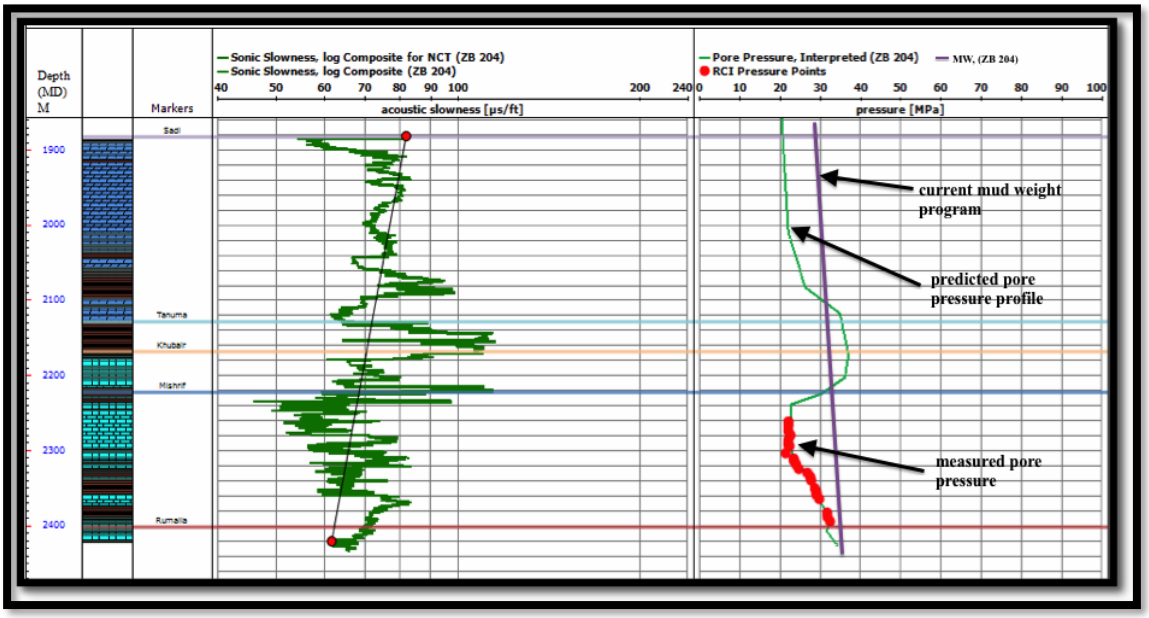

Figure 6b. Pore pressure profile in well ZB 204.

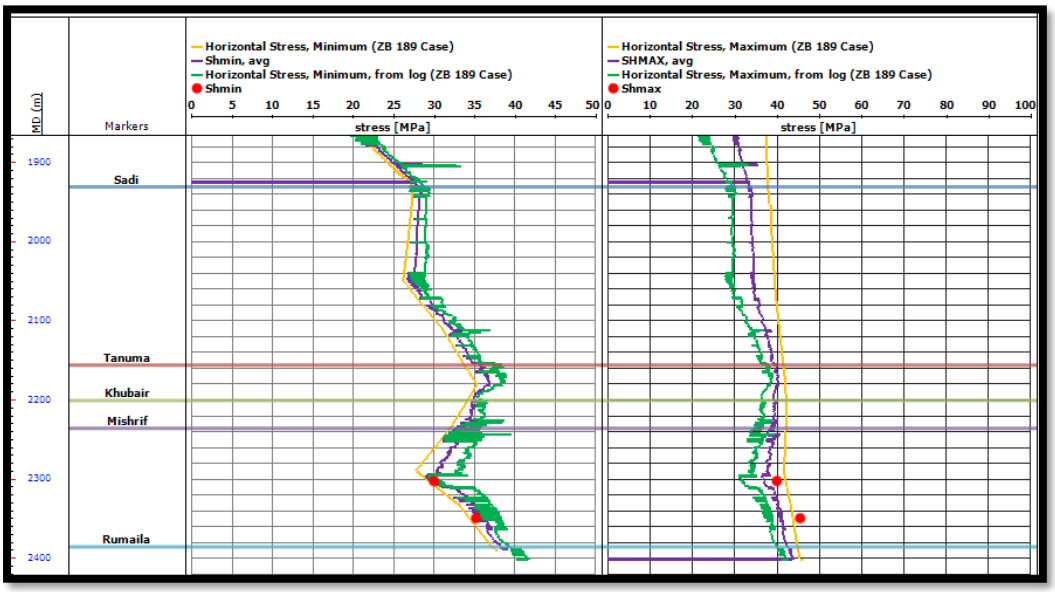

Figure 7a. Minimum and Maximum horizontal stress profiles in well ZB 189.

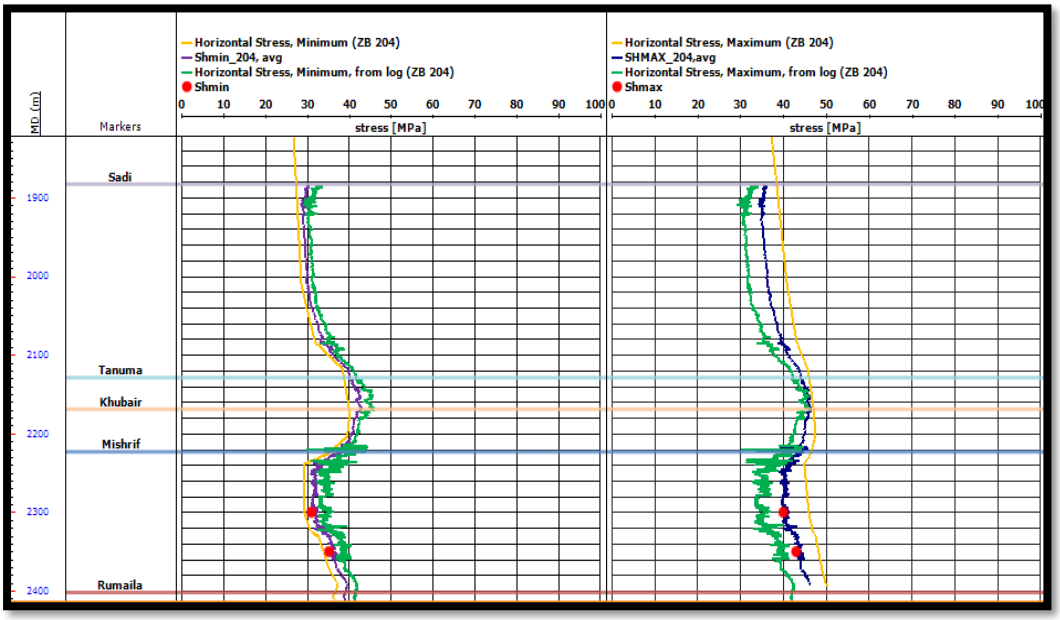

Figure 7b. Minimum and Maximum horizontal stress profiles in well ZB 204.

The trend line between these two points is then calculated, which creates a trend line-based log, which will be used to calculate the complete horizontal stress profile.

The Stress Contrast method provides a means for stress calculations from logs and considering an isotropic tectonic strain with Biot coefficient equal to 1, Eq. (13a) and Eq. (13b),

$$S_{hmin} = \left(\frac{\nu}{1-\nu}\right)(S_v - P_p) + P_p + \left(\frac{1+\nu}{1-\nu^2}\right)E\varepsilon \quad (13a)$$

$$S_{Hmax} = \left(\frac{\nu}{1-\nu}\right)(S_v - P_p) + P_p + \left(\frac{1+\nu}{1-\nu^2}\right)E\varepsilon \quad (13b)$$

The difference between Eq. (13a) and Eq. (13b) is in the value of the strain constant (ε) and they are (1×10^{-4} for S_{hmin} and 5×10^{-4} for S_{Hmax}). Moreover, the average profile of both curves is used for the consequent calculations.

3.2.4 Orientation of Horizontal Stresses:

In vertical wells, direction of SHmax is perpendicular to the direction of Shmin. By analyzing the breakouts on the available resistivity image logs **(Fig. 8)**, the direction of Shmin is at an azimuth of 290° with an orientation to NW-SE giving the direction of SHmax as 200° NE-SW.

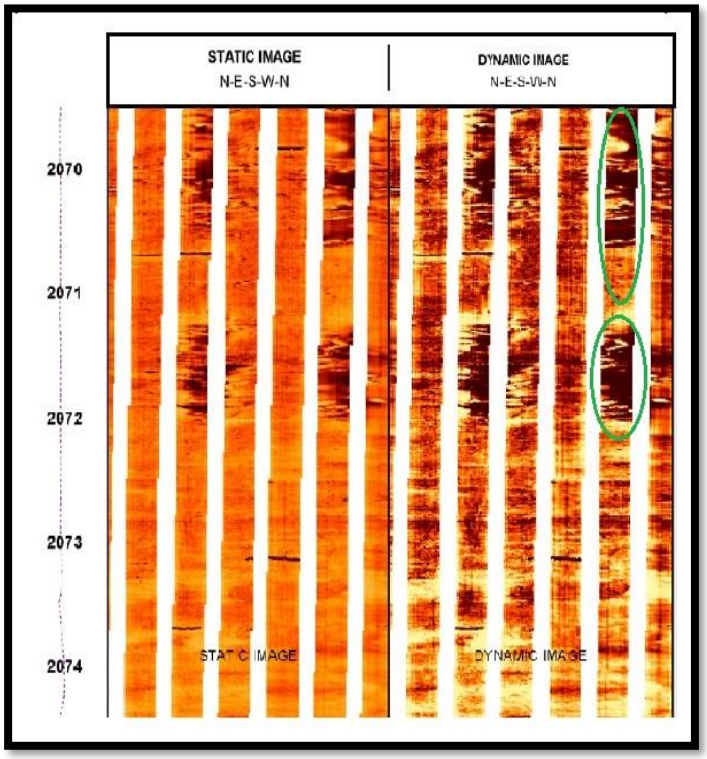

Figure 8. Breakouts (highlighted in green), shown by XRMI Image Log.

3.3 Fracture Pressure Prediction:

Fracture pressure was predicted using Hubbert and Willis formula, Eq. (14), for both wells. The basis for this formula is that the sum of the formation pore pressure and the effective stress equals the total overburden pressure. Results are shown in **(Fig. 9a and 9b)**.

$$P_F = P_p + 0.5(S_v + P_p) \quad (14)$$

where,
P_F is the Fracture Pressure.

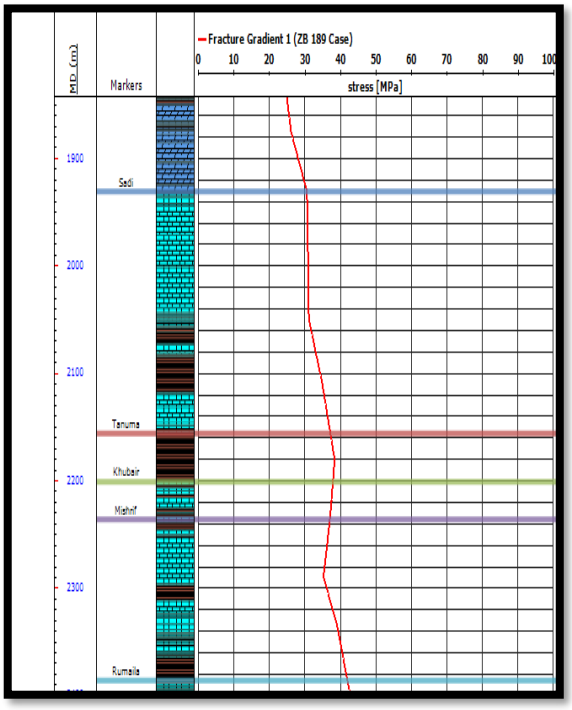

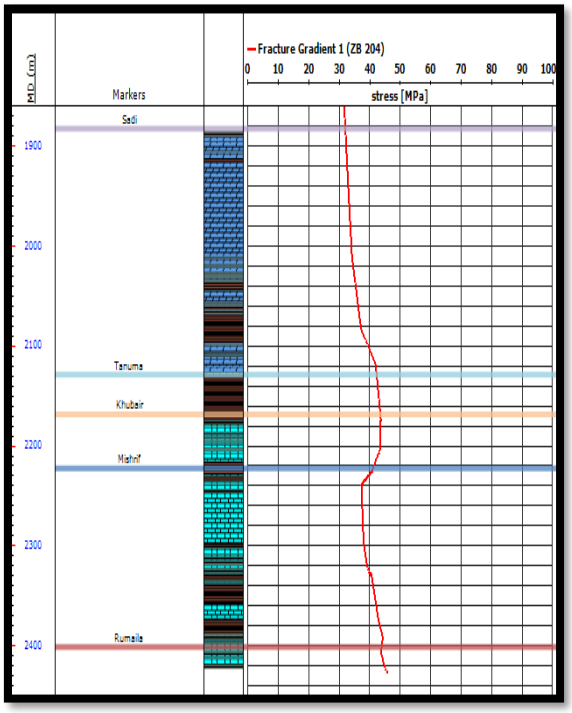

Figure 9a. Fracture Pressure profile in well ZB 189. **Figure 9b.** Fracture Pressure profile in well ZB 204.

Displaying all results in a single diagram will help us to get better understanding of what is going on and how stresses related to each other. It also helps us to spot and diagnose possible problem and therefore to suggest better decisions and solutions. Therefore, results of both wells are displayed in **Fig. 10**.

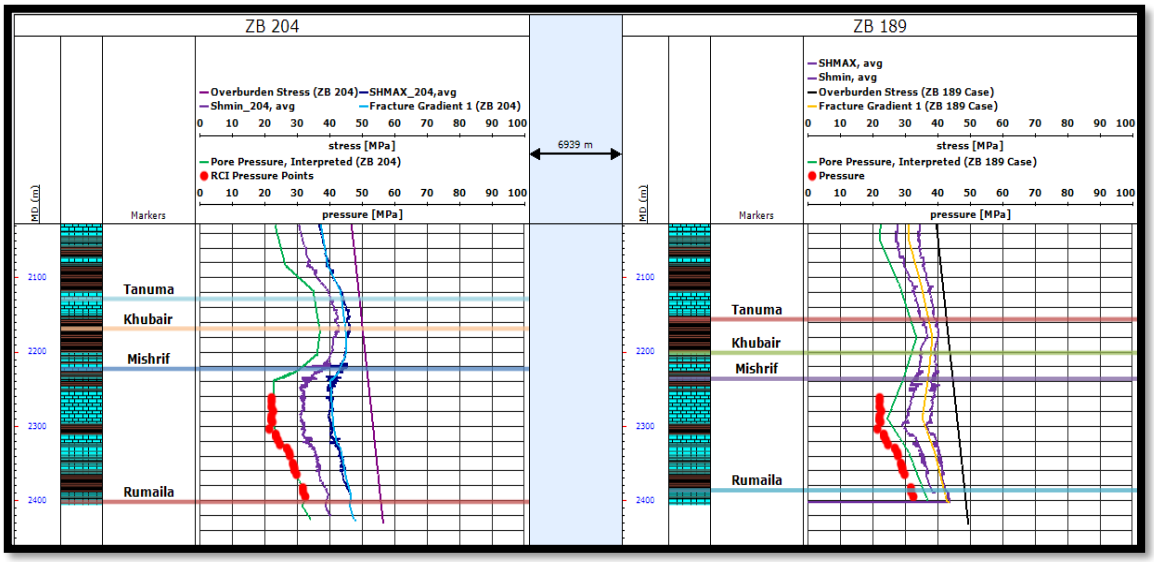

Figure 10. 1D MEM Results in both wells.

Due to the lack of core measurements, a sensitivity analysis using quantitative risk assessment (QRA) and tornado plot are conducted. A tornado plot **(Fig. 11)** lists the most important parameters that affect the fracture breakdown pressure which will lead to the unwanted breakouts. The results

shows that the minimum horizontal stress has the bigger influence on the rock failure since it is chosen as the upper bound of the mud window.

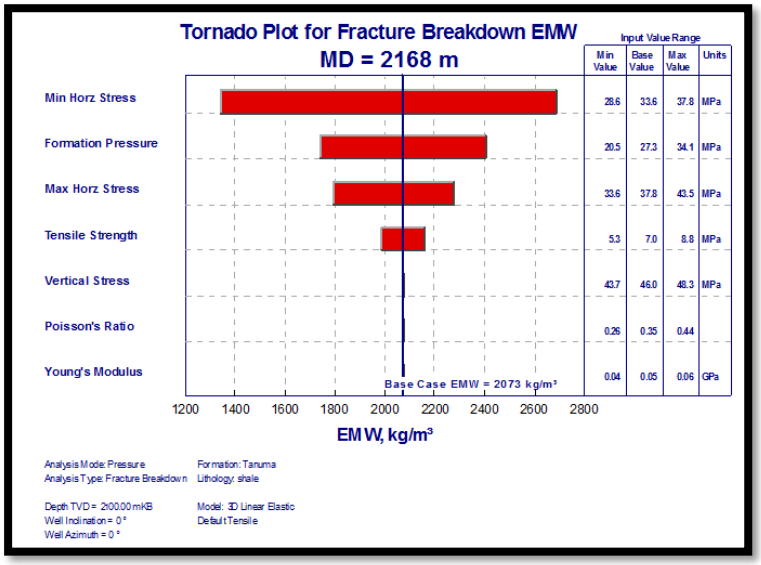

Figure 11. Sensitivity analysis using Tornado plot for Tanuma formation.

Quantitative risk assessment **(Fig. 12)** also showed the probability of success for the mud window at Tanuma formation. This analysis clearly shows the probability of success for three cases (P10, P50 and P90) at the depth of 2168m. The probability of success means the mud window available at that depth without exposing the formation to any failure.

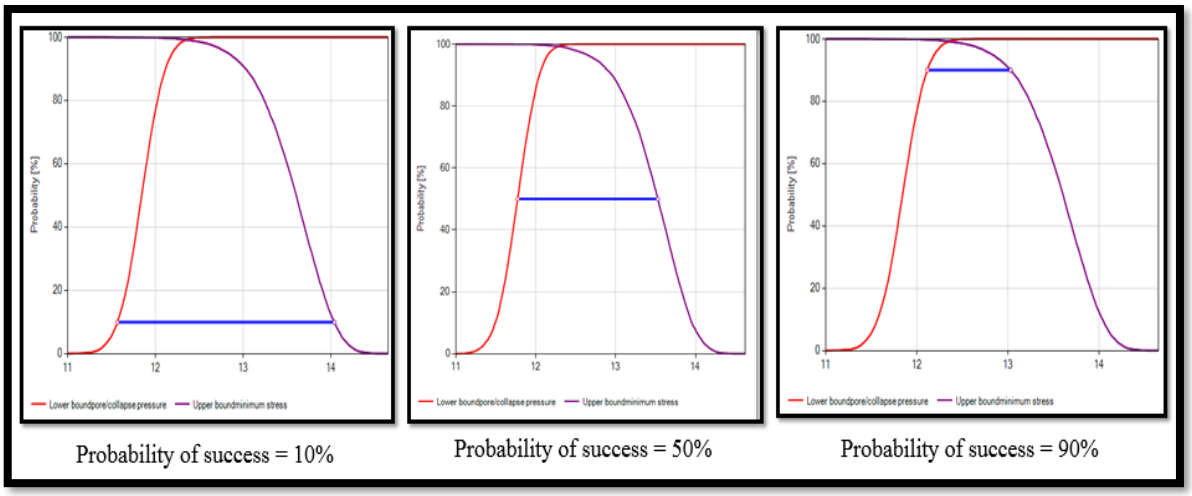

Figure 12. Sensitivity analysis using QRA for Tanuma formation.

Results for each probability are shown in **Table 2**.

Table 2. Probability of success for allowable mud weight results.

Probability of success	Allowable Mud Weight, ppg	
	Lower	Upper
P10	11.5	14.2
P50	11.8	13.6
P90	12.2	13.1

Increasing the probability of success means increasing the risk, thus depending on the experience of the region and -if available- similar cases from nearby fields is necessary.
In addition, as from the sensitivity analysis results, it is highly important to conduct rock experiments and leak-off test for Zubair oilfield for calibrating the mechanical earth model and thus a better results for mud program selection may be obtained, which leads to less wellbore instability problems thus reduction in the non-productive time.

3.4 Conclusions

- In this study, the results of 1D Mechanical Earth Model show an increase in pore pressure and in both maximum and minimum horizontal stresses in the interval from 2075m (lower parts of Sadi formation) to 2225m (upper part of Mishrif formation).
- The transition zone of the increase in pore pressure was considered from 2075m to 2125m. Zone of over pressure was noticed from 2125m to 2200m in Tanuma shaly formation, which known for its increase in over pressure in the southern part of Iraqi oilfields. Pore pressure starts back to hydrostatic in a gradual manner from 2200m to 2225m.
- Based on the analysis of XRMI image logs, the orientation of minimum horizontal stress is NW-SE with an azimuth of 290^{o}; this gives the maximum horizontal stress an orientation in the NE-SW with an azimuth of 200^{o}. Orientation of both horizontal stresses provides a trajectory plan for drilling directional wells in future development plans.
- Wells tornado plot shows that the minimum horizontal stress has the bigger effect on the results and because the minimum horizontal stress model depends on Poisson ratio in its calculation, an emphasis should be made again on performing laboratory core tests to provide the needed calibration data.
- Based on the sensitivity analysis results and due to the narrow mud weight window, the applicability of using the managed pressure drilling (MPD) or Annular Pressure While Drilling (APWD) techniques should be checked in a situation where narrow mud window encountered.

Acknowledgements:
This paper would not have been possible without all the support and the encouraging words from my supervisor Dr. Nada S. Al-Zubaidi, to the department of Petroleum Engineering / College of Engineering/ University of Baghdad, and to the Ministry of Oil.

REFERENCES:

- Abbood, H. R., 2016. 'Mitigation Of Wellbore Instability In Deviated Wells By Using Geomechanical Models And Mpd Technique', Master thesis.
- Alkamil, E. H. K. and Abbood, H. R., 2018. 'SPE-192359-MS Using Managed Pressure Drilling to Reduce Stuck Pipe Problem MPD or UBD MPD Strategy to Reduce Stuck Pipe Risk'.
- Amani, M. et al., 2010. 'Using Drilling and Logging Data for Developing 1D Mechanical Earth Model for a Mature Oil Field to Predict and Mitigate Wellbore Stability Challenges', pp. 1–12. doi: 10.2523/132187-ms.
- V. Fattahpour, A. Pirayehgar, M.B. Dusseault, B. M., 2012. 'Building a Mechanical Earth Model : a Reservoir in Southwest Iran', pp. 1–8.
- Fischer, K., 2013. Geomechanical reservoir modeling – workflow and case study from the North German Basin. Technische Universität Darmstadt.
- Gholami, R. et al., 2014. 'Practical application of failure criteria in determining safe mud weight windows in drilling operations', Journal of Rock Mechanics and Geotechnical Engineering. Taibah University, 6(1), pp. 13–25. doi: 10.1016/j.jrmge.2013.11.002.
- Goodman, H. E. and Connolly, P., 2007. 'Reconciling subsurface uncertainty with the appropriate well design using the mechanical Earth model (MEM) approach', The Leading Edge, 26(5), pp. 585–588. doi: 10.1190/1.2737098.
- Horsrud, P., 2007. Estimating Mechanical Properties of Shale From Empirical Correlations', SPE Drilling & Completion, 16(02), pp. 68–73. doi: 10.2118/56017-pa.
- Jizba, D. L., 1991. 'Mechanical and acoustical properties of sandstones and shales', Stanford University, p. 275.
- Kidambi, T. and Kumar, G. S., 2016. 'Mechanical Earth Modeling for a vertical well drilled in a naturally fractured tight carbonate gas reservoir in the Persian Gulf', Journal of Petroleum Science and Engineering. Elsevier, 141, pp. 38–51. doi: 10.1016/j.petrol.2016.01.003.
- McNally, G. H., 1987. 'Estimation of coal measures rock strength using sonic and neutron logs', Geoexploration, 24(4–5), pp. 381–395. doi: 10.1016/0016-7142(87)90008-1.
- Moazzeni, A. R. et al., 2010. 'Mechanical Earth Modelling Improves Drilling Efficiency and Reduces Non-Productive time (NPT)'. doi: 10.2118/131718-ms.

- Plumb, R. et al., 2000. 'IADC / SPE 59128 The Mechanical Earth Model Concept and Its Application to High-Risk Well Construction Projects', IADC/SPE Drilling Conference, pp. 1–13.

- Sirat, M., Ahmed, M. and Zhang, X., 2015. 'Predicting Hydraulic Fracturing in a Carbonate Gas Reservoir in Abu Dhabi Using 1D Mechanical Earth Model: Uncertainty and Constraints', pp. 1–11. doi: 10.2118/172942-ms.